Communication

Vectorial Manipulation of High-Resolution Focusing Optical Field through a Scattering Medium

Bote Qi, Lihua Shen, Khian-Hooi Chew and **Rui-Pin Chen** *

Key Laboratory of Optical Field Manipulation of Zhejiang Province, Department of Physics, Zhejiang Sci-Tech University, Hangzhou 310018, China
* Correspondence: chenrp@zstu.edu.cn

Abstract: The manipulation of the polarization states of the light transmitted through a scattering medium has become an emerging field due to the novel fundamental physics interest and potential applications. Here, the manipulation of the polarization states in the focusing high-resolution optical field (points and vector beams) after passing a scattering medium is theoretically and experimentally demonstrated. The vector transmission matrix (VTM) of a scattering medium is measured with the vector basis of orthogonally circular polarizations by the two-dimensional (2D) holographic grating combined with the four-step phase-shifting method. The incident wavefronts for the creation of desired high-resolution optical fields through a scattering medium are modulated according to the calculation with the VTM of the medium. The theoretical and experimental results show that the constructed high-resolution optical field with spatially variant states of polarization can be realized through frosted glass. These results provide a new way to vectorially manipulate the constructed high-resolution optical field by passing through a scattering medium.

Keywords: vector beams; scattering medium; vector transmission matrix; phase shift method; 2D holographic grating

1. Introduction

As an important parameter of light, the manipulation of the polarization states has attracted a lot of attention. In particular, the technology for manipulating the polarization states of the light transmitted through a scattering medium can be applied to polarization-sensitive optical coherence tomography [1] and various coherent nonlinear microscopy techniques [2]. On the other hand, vector beams have attracted increasing interest due to their spatially inhomogeneous polarization states [3]. The novel properties of a vector beam have found potential applications in optical trapping [4,5], laser cutting [6], high-resolution imaging [7], and optical communication [8]. However, most of these studies do not take into account the phase aberrations and depolarization effects that may be experienced during the propagation of vector beams in a medium with nonuniform index distributions. The phase, amplitude, and polarization information of the incident beams will be disturbed when they propagate through a scattering medium, leading to a great impact on the quality of imaging and the transmission of useful information [9,10]. Numerous techniques have been proposed to overcome the scattering effect and achieve the transmission of light beams through a scattering medium, such as an optical transmission matrix [11–19], optical phase conjugation imaging [20,21], and the speckle correlation technique [22–24]. Furthermore, these techniques have been applied to light beam subdiffraction focusing [25], deep biological tissue imaging [26], etc. Recently, the vector transmission matrix (VTM) has been proposed to characterize the deterministic relationship of the amplitude, phase, and polarization state between the input light fields and output light fields through a scattering medium [27]. Although, the measurement of VTM of a scattering medium and polarization control in a single focus point by the experimental system has been explored [27,28], the

measurement processes of VTM are relatively complicated. The generation of multiple focal spots and vector beams with spatially varying states of polarization after passing through a scattering medium has been theoretically demonstrated [29]. More recently, the generation of vector beams with a scattering medium by one single scalar transmission matrix has been proposed [30]. However, the simultaneous vector manipulation of the states of polarization in both azimuthal and radial directions after passing through a scattering medium needs further exploitation, especially for the input optical field with different orthogonal polarizations such as left- and right-circular polarizations.

In this work, we present a simple and reliable method to manipulate the spatial distribution of polarization state in both azimuthal and radial directions in the focusing high-resolution optical field (points and vector beams) after passing through a scattering medium. In particular, the input optical field with a vector beam by special polarization superposition of orthogonally circular polarizations can provide feasibility to achieving such a vectorial manipulation process. The desired high-resolution optical field with spatially varying states of polarization is experimentally generated through the scattering medium by using the VTM with the vector basis of the orthogonally circular polarizations. The VTM of the scattering medium is measured with the spatial light modulator (SLM) and a $4f$ optical system without moving the experiment devices, which greatly reduces the phase measurement error of the VTM. In addition, compared to the conventional method for a high-resolution focusing optical field with orthogonally linear polarizations [27,28], the vectorial manipulation of the desired optical field through a scattering medium with the vector basis of left- and right-hand circular polarizations has an advantage in focusing precision and quality compared to that with orthogonally linear polarizations [31,32].

2. Measurement of the Vector Transmission Matrix

According to the concept of the Jones vector, any vector beam can be expressed as a linear combination of the complex amplitudes of two orthogonal polarization components [33]. The input and output vector light field through a scattering medium can be defined as the coherent superposition of two orthogonally circular polarizations:

$$\vec{E}_{in} = \begin{bmatrix} E_{in,l}(m,n) \\ E_{in,r}(m,n) \end{bmatrix}, \ \vec{E}_{out} = \begin{bmatrix} E_{out,l}(p,q) \\ E_{out,r}(p,q) \end{bmatrix} \tag{1}$$

where E_{in} (m,n) and E_{out} (p,q) are, respectively, the Jones vector of the (m,n) point in the input plane and the (p,q) point in the output plane. $E_{in,l}$ and $E_{in,r}$ represent the complex amplitudes of the left- and right-hand circular polarizations, respectively. $E_{out,l}$ and $E_{out,r}$ are the corresponding complex amplitudes of the left- and right-hand circular polarizations in the output plane, respectively. The relationship between the input and output light fields can be expressed as:

$$\vec{E}_{out} = \begin{bmatrix} E_{out,l}(p,q) \\ E_{out,r}(p,q) \end{bmatrix} = \sum_{m,n,p,q} \begin{bmatrix} T_{ll}(m,n,p,q) & T_{lr}(m,n,p,q) \\ T_{rl}(m,n,p,q) & T_{rr}(m,n,p,q) \end{bmatrix} \begin{bmatrix} E_{in,l}(m,n) \\ E_{in,r}(m,n) \end{bmatrix} \tag{2}$$

The VTM of a scattering medium can be defined as T. For highly polarization-sensitive anisotropic scattering media such as ZnO scattering layers, the polarization state of the input field is multiply scattered and perturbed. The components T_{ll}, T_{lr}, T_{rl} and T_{rr} in the VTM should be considered [28]. On the other hand, for an isotropic scattering medium such as the frosted glass used in this work, the components of the VTM for the isotropic scattering medium usually have the properties of $T_{rl} = 0$ and $T_{lr} = 0$ [34]. Therefore, the VTM can be simplified as:

$$T = \sum_{m,n,p,q} \begin{bmatrix} T_{ll}(m,n,p,q) & 0 \\ 0 & T_{rr}(m,n,p,q) \end{bmatrix} \tag{3}$$

The size of the VTM is 2M × 2N and the VTM contains two subscalar transmission matrices (M and N, respectively, represent the total number of elements on the output and input surfaces). The information content of the VTM to be measured is two times that of the scalar transmission matrix.

The experiment system for the measurement of the VTM and the generation of an arbitrary vector beam through the scattering medium is shown in Figure 1. The experiment setup is composed of two parts: (i) the optical-field-manipulating system and (ii) the scattering imaging system. The optical-field-manipulating system consists of the 4*f* system, a spatial light modulator (SLM), two Fourier lenses (L3 and L4), a spatial filter (F), two λ/4 wave plates, and a Ronchi grating (G). The scattering imaging system consists of the two objective lenses (O1, 10× and O2, 20×, Hengyang Optics, Guangzhou, China) a scattering medium (S, frosted glass of 220 mesh, LBTEK, DW105-220. The glass sheet is polished and sanded to obtain the frosted glass [35]), and an image sensor (CMOS). The core function of the optical field manipulating system is the manipulation of the polarization and phase of the input optical field. The +1 orders of the *x*-axis and *y*-axis on the spectrum plane after reflecting by the SLM are extracted by a double-hole filter and are converted into left-hand and right-hand circular polarizations through the λ/4 wave plates close to each hole, and generate the required vector beams through the collinear superposition of the left-hand and right-hand circular polarizations by G [36]. Therefore, the input optical fields with different distributions of polarization and phase are dependent on the loaded holograms on the SLM. Note that the left- and right-hand circularly polarized components are adopted as the input basis vectors to generate a vector beam through a scattering medium. The measurement of the VTM is also divided into two parts with respect to the orthogonal circular polarizations, as demonstrated above. In the imaging system, the input light is focused on the scattering medium S by the objective lens O1; then, the scattered light passing through the scattering medium S is collected by the objective lens O2 and transmitted to the CMOS plane with the speckle intensity map. A CMOS (Daheng Optical MER2-302-56U3M with a pixel size of 3.45 μm) with 2548 × 1536 pixels is adopted to record the intensity map of scattered light in the output plane after passing through the scattering medium, and the 200 × 200 pixels in the center of the CMOS are taken as the effective sampling area for measuring VTM. To calibrate the VTM, the phase-shifting method and a 2D holographic grating are applied.
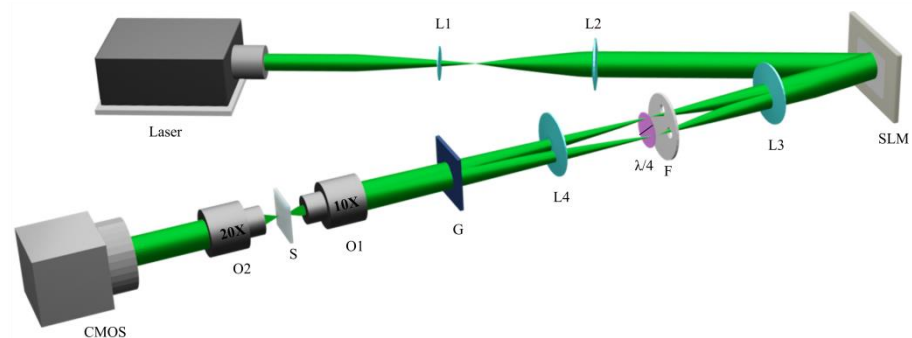

Figure 1. Schematic of the experimental setup for measuring the complex VTM and the generation of an arbitrary vector beam through a scattering medium where: SLM—spatial light modulator; O1 and O2—objective lenses; G—Ronchi grating; S—scattering medium (frosted glass of 220 mesh); F—spatial filter; L1, L2, L3, and L4—lenses.

The input field is modulated by a 2D holographic grating displayed on the SLM with the 2D modulation function as [37]:

$$t(x,y) = \left(1 + \frac{\gamma}{2}\cos(2\pi f_0 x + \delta_1(x,y)) + \frac{\gamma}{2}\cos(2\pi f_0 y + \delta_2(x,y))\right) \tag{4}$$

where $\delta_1(x,y)$ and $\delta_2(x,y)$ are the phase structures carried by the left- and the right-hand circular polarization, respectively. f_0 is the spatial carrier frequency, and γ is the

modulation depth. The SLM is divided into a central control region and a peripheral reference region [11,12]. The peripheral area is used for the reference signal required for interferometry when measuring VTM. The control area is divided into 1024 independently controllable segments. To improve the ratio of signal to noise of the output field in the CMOS after passing through the scattering medium, the Hadamard basis is adopted by using the four-step phase-shift method to measure the VTM [11,12,27]. When measuring the VTM, the Hadamard basis as the additional phase of the input light field to encode its phase information into 2D holographic grating with the modulating function as:

$$t(x,y) = \left(1 + \frac{\gamma}{2}\cos\left(2\pi f_0 x + \delta_p(x,y)\right) + \frac{\gamma}{2}\cos(2\pi f_0 y)\right) \qquad (5)$$

where $\delta_p(x,y)$ is the phase of the Hadamard basis. Each column of the Hadamard matrix is used as the input mode, the additional phases 0, $\pi/2$, π, and $3\pi/2$ are added sequentially in the input mode according to the four-step phase-shifting method [12], and the corresponding elements of the T_{ll} were calibrated by measuring the corresponding input mode. The components of the VTM T_{rr} can also be measured in the same way; therefore, the full components of VTM of frosted glass can be obtained.

Once the full VTM is known, the arbitrary vector beams with a spatially variant state of polarization can be obtained through the scattering medium. Here, the experiments are further carried out to construct vector beams with spatially variant states of polarization by passing through the scattering medium. The matrix operations between the input and output components of the light field are calculated as:

$$\left[\begin{array}{c} E_{in,l}(m,n) \\ E_{in,r}(m,n) \end{array}\right] = \sum_{m,n,p,q} \left[\begin{array}{cc} T_{ll}(m,n,p,q) & 0 \\ 0 & T_{yy}(m,n,p,q) \end{array}\right]^* \left[\begin{array}{c} E_{target,l}(p,q) \\ E_{target,r}(p,q) \end{array}\right] \qquad (6)$$

where '*' stands for the conjugate operation. E_{target} is a target area of an output optical field. The input light fields $E_{in,l}$ and $E_{in,r}$ can be calculated by Equation (6), and the phase information can be extracted as δ_x and δ_y. Furthermore, to overcome the scattering effect, the additional phases δ_x and δ_y are encoded into a 2D holographic grating in the SLM to modulate the wavefront phase of the left-hand and right-hand circular polarization. Therefore, the modulating function of the 2D holographic grating in the SLM is expressed as:

$$t(x,y) = \left(1 + \frac{\gamma}{2}\cos(2\pi f_0 x + \delta_1(x,y) + \delta_x(x,y)) + \frac{\gamma}{2}\cos\left(2\pi f_0 y + \delta_2(x,y) + \delta_y(x,y)\right)\right) \qquad (7)$$

When the 2D holographic grating is loaded into the SLM, the phases $\delta_1 + \delta_x$ and $\delta_2 + \delta_y$ will be imposed into the left-hand and right-hand circular polarizations in the sequent experiment procedure, respectively, and the desired vector beam with a spatially variant state of polarization can be obtained after passing through the scattering medium.

3. Result Analysis

Firstly, the manipulation of the spatially variant states of polarization of the single focusing points through the scattering medium by using the measured VTM is theoretically and experimentally demonstrated. The theoretical and experimental results of the intensity distributions of the focusing spots with a different state of polarization after passing the scattering medium are tested with or without the different polarization analyzers, as shown in Figure 2. Figure 2a–c show the constructed single focusing points with the left-hand circular, right-hand circular, and vertically linear polarizations after passing through the scattering medium. Furthermore, the simultaneous manipulation of multi-focusing-points with different polarization states is realized by using the VTM; the right-hand circular, vertically linear, and left-hand circular polarizations occur at the left, middle, and right points, respectively, as shown in Figure 2d. These results provide a novel way to manipulate the polarization in the high-resolution focusing points.
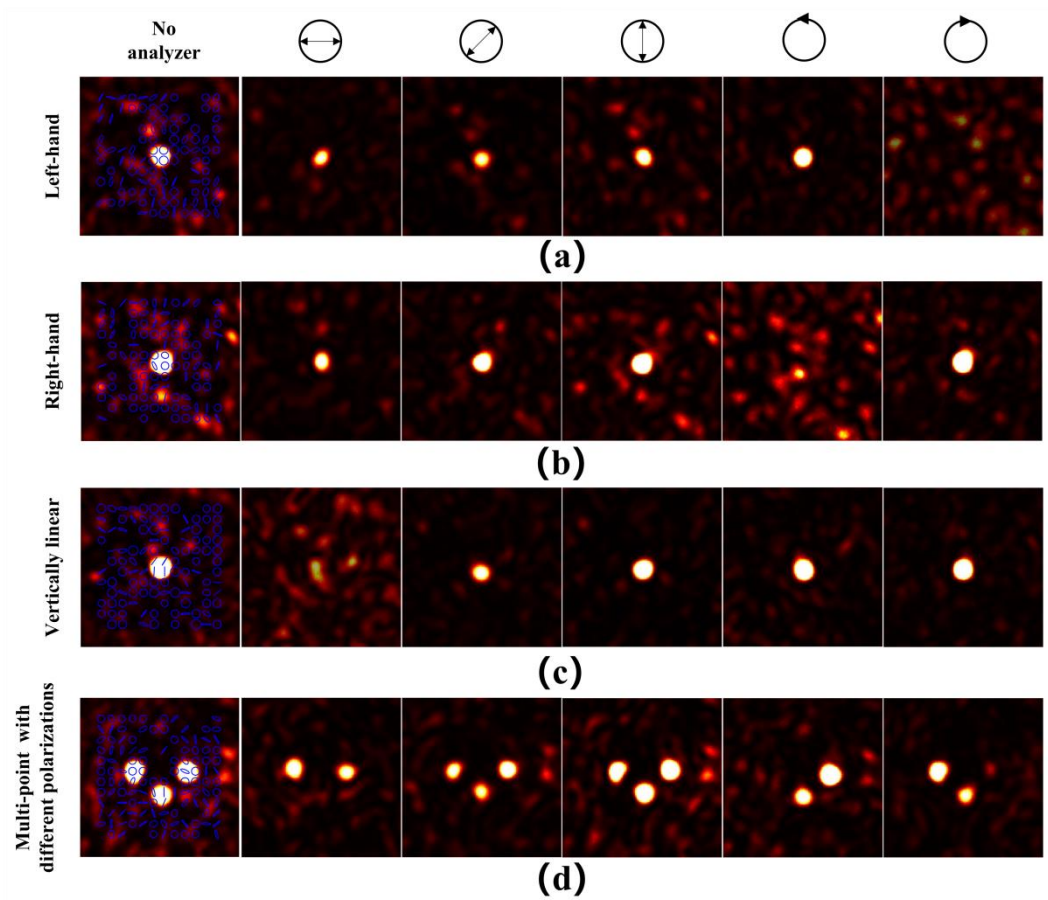
Figure 2. The intensity distribution of focusing spots with different states of polarization (**a**) left-hand circular polarization; (**b**) right-hand circular polarization; (**c**) vertically linear polarization; (**d**) three focusing points with left-hand circular, right-hand circular and vertically linear polarization, respectively. Here, the sizes of each plot are $517 \times 517 \ \mu m^2$.

The high-resolution effect of the optical field through the scattering medium has become a breakthrough technology in the imaging field [38,39]. The high-resolution effect generated due to the higher frequency components of the angular spectrum of the optical field scattered by the scattering medium can be collected in the focusing region [40]. The high-resolution effect of the scattering medium also can contribute to the generation of high-resolution vector beams after passing through a scattering medium.

Besides the manipulation of the polarization in the high-resolution focusing points, the generation of vector beams through a scattering medium can be also realized. A vector beam with spatially variant states of polarization in both radial and azimuthal directions can be described as:

$$\vec{E}(r,\varphi) = A_0 \left(\cos\left(\frac{2\pi l r}{r_0} + m\varphi \right) \vec{e}_x + \sin\left(\frac{2\pi l r}{r_0} + m\varphi \right) \vec{e}_y \right) \qquad (8)$$

where φ is the azimuthal angle in the polar coordinate system, m is the polarization topological charge number, r_0 is the radius of the aperture-truncated beam, and l is the radially modulating parameter. Note that the state of polarization described by Equation (8) is a locally linear polarization in the cross-section of the vector beam; thereafter, the state of polarization is examined by a linear polarizer. Without a scattering medium, the vector beams can be generated in the first part of the experiment setup (see Figure 1) with the modulating function of the 2D holographic grating displayed on the SLM as Equation (4). If the vector beams become the desired output field after passing through the scattering medium, then the modulating function of the 2D holographic grating displayed on the

SLM should be described as Equation (7) with the δ_x and δ_y dependent on the VTM of the scattering medium.

The simulating and experiment results with different topological charge numbers and radially modulating parameters are shown in Figure 3. Note that, hereafter, a scattering VTM with random phase distribution is adopted to simulate a scattering medium for the theoretical calculations [29]. Figure 3a–c show the intensity distributions of the total field and different polarization components for the cases $m = 1, 2, 3$ and $l = 0$. The corresponding intensity distributions with $m = 0, l = 1$ are shown in Figure 3d. A good agreement between the simulation and experiment results for the polarization state distribution of constructed vector beams was observed, as shown in Figure 3. It further proves that the polarization information of the constructed vector light field can be accurately manipulated through a scattering medium.
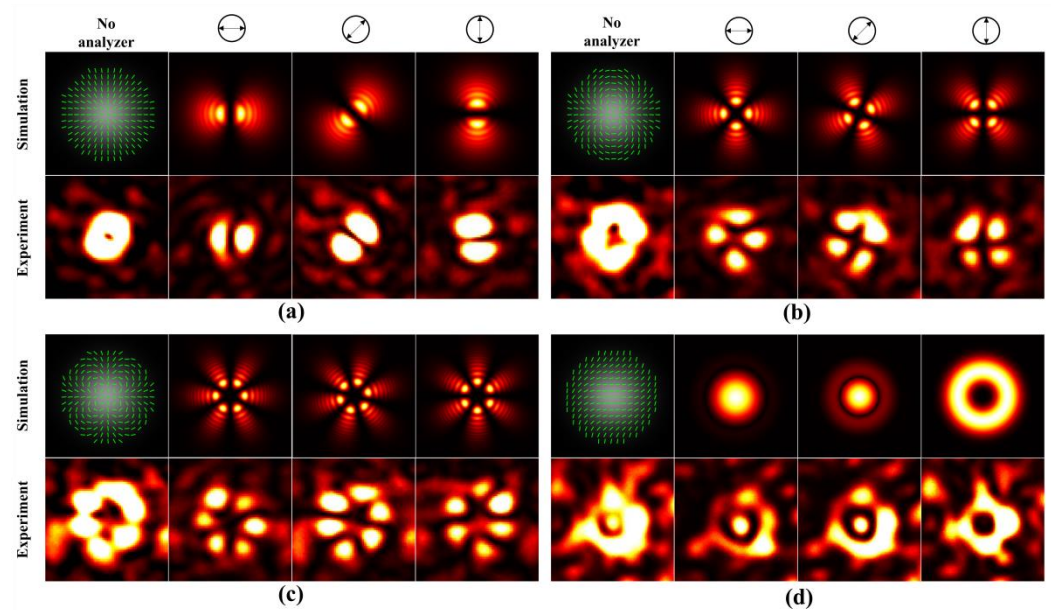

Figure 3. Simulation and experiment results for the intensity distributions of constructed vector beams through a scattering medium. The parameter values are: (**a**) $m = 1, l = 0$; (**b**) $m = 2, l = 0$; (**c**) $m = 3, l = 0$; (**d**) $m = 0, l = 1$. In each case, the total, horizontal, 45° and vertical intensity distributions are in sequence from left to right. The polarization state distributions of the beam are shown in the first plot in each panel. Here, the sizes of each plot in (**a**–**c**) are $220 \times 220 \ \mu m^2$, and the sizes of each plot in (**d**) are $414 \times 414 \ \mu m^2$.

In addition, the experimental results in this work by the proposed method indicate that the vectorial manipulation of the desired optical field through a scattering medium with the vector basis of left-hand and right-hand circular polarizations has an advantage in focusing precision and quality compared to that with orthogonally linear polarizations (the results with orthogonally linear polarizations are not shown here). Furthermore, the manipulation of the more complex polarization state in both radial and azimuthal directions after passing through the scattering medium is also analyzed and verified. The simulation and experimental results for the intensity distributions of the complex vector beam generated through a scattering medium are shown in Figure 4. Figure 4a,b present the constructed vector beams with states of polarization $m = 1, l = -1$ and $m = -1/2, l = 1$ (see Equation (8)), respectively. The states of polarization of the constructed vector beams are examined by a linear polarizer, the experimental results are consistent with the simulation results for the vector beams as shown in Figure 4. Therefore, the results provide evidence that the complex polarization state of a vector beam through a scattering medium can be constructed with the VTM method.
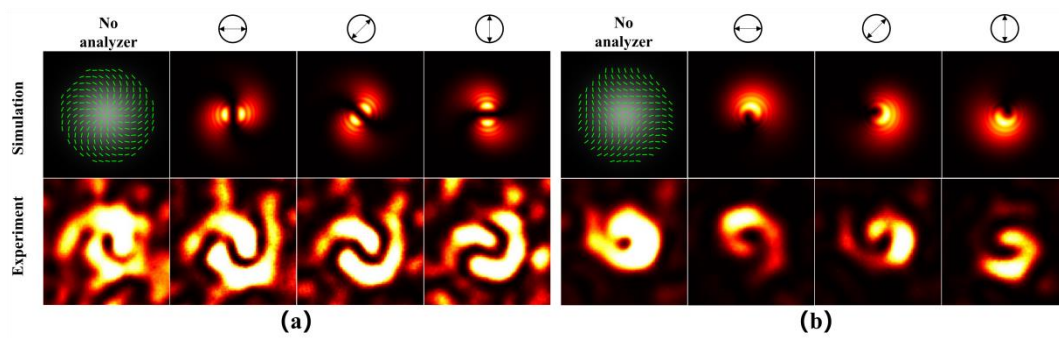
Figure 4. Simulation and experiment results for the intensity distributions of constructed complex vector beam generation through a scattering medium: (**a**) $m = 1$, $l = -1$ (**b**) $m = -1/2$, $l = 1$. The polarization state distributions of the beam are shown in the first plot in each panel. Here, the sizes of each plot are 345×345 μm^2.

In particular, the high-resolution effect of the scattering medium for the constructed vector beams is described in Figure 5. In Figure 5, the focusing vector beams with $m = 1, 2$ and 3 are generated and compared by the optical system with and without the scattering medium (see Figure 1 for the experiment procedure). The intensity distributions of the vector beams with $m = 1, 2$ and 3 focused by a conventional lens with a focal length of 100 mm are shown in Figure 5a, whereas the intensity distributions through the scattering medium (frosted glass of 220 mesh) are presented in Figure 5b, and the zoom of the intensity distributions in the central parts of Figure 5b are described in Figure 5c. The scattered light through the scattering medium (frosted glass of 220 mesh) can achieve a vector focusing effect 10 times more than that of the traditional lens focusing, as shown in Figure 5.
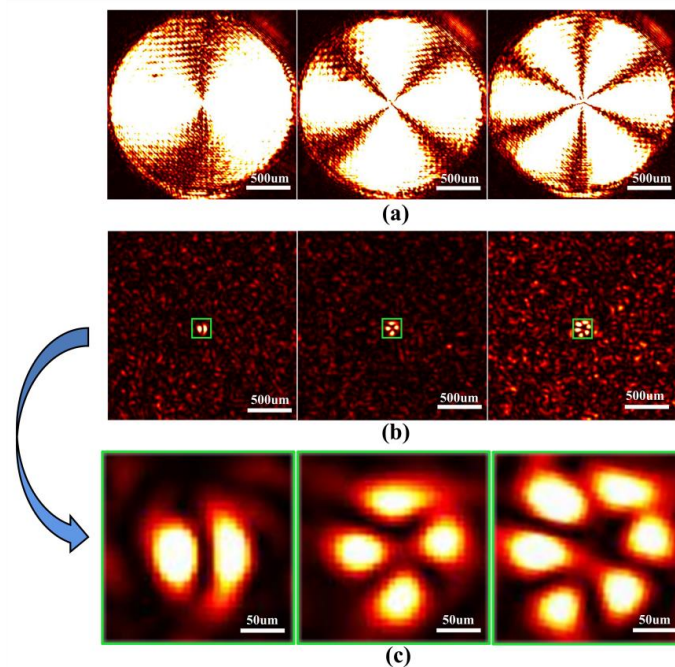

Figure 5. (**a**) The intensity distributions of the vector beams with $m = 1, 2,$ and 3 focused by a conventional lens with a focal length of 100 mm. (**b**) the intensity distribution of the vector beams with $m = 1, 2,$ and 3 generated by our scattering imaging method. (**c**) all the plots are $10\times$ magnification of the intensity distributions in central parts of (**b**). The above plots are recorded when the polarization analyzer is oriented horizontally. The scale bar is 500 μm (in the recording plane). The sizes of each plot in (**a,b**) are 1725×1725 μm^2, and the sizes of each plot in (**c**) are 172.5×172.5 μm^2.

4. Discussion

The interaction of an optical vector field with scattering media, especially the manipulation of the state of polarization of the focusing high-resolution optical field after passing through a scattering medium, is an important and interesting topic. This proposed method using a vector beam with the coherent superposition of orthogonally circular polarizations provides feasibility of achieving the vectorial manipulation of the spatial distribution of polarization state in the focusing high-resolution optical field (points and vector beams) after passing through a scattering medium in both azimuthal and radial directions. Because the orthogonally circular polarizations can be flexibly managed by SLM and $4f$ optical system, the spatially variant state of polarization of the focusing high-resolution optical field after passing through a scattering medium is purposely manipulated.

In addition, compared to the input vector optical field with the superposition of orthogonally linear polarization, our experiment results indicate that the focusing optical field after passing through a scattering medium with the orthogonally circular polarizations has an advantage in the robustness of the polarization state and field distributions. Figure 6 shows the comparison of the focusing optical field between the input vector beams with orthogonally linear and circular polarizations; the vector optical field constructed by the orthogonally linear polarizations can be expressed as $\vec{E}(r, \varphi) = A_0 \left(\cos(2\pi lr/r_0 + m\varphi)\vec{e}_x + \sin(2\pi lr/r + m\varphi)\vec{e}_y \right)$ [37]. Although the memory effect has been observed in the backscattering geometry of light interacting with a random medium [31,32,41], the underlying physics for the difference between the circular and linear polarizations passing through a scattering medium, need to be further exploited.
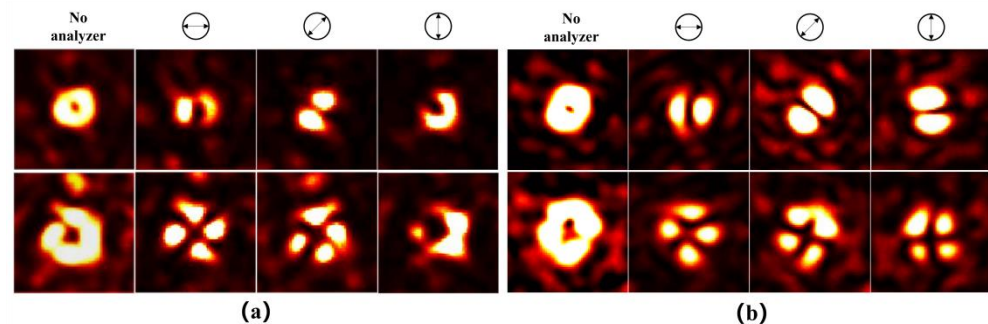

Figure 6. Comparison between the experimental results for the intensity distributions of vector beam constructed using orthogonally linear polarizations and orthogonally circular polarizations: (**a**) $m = 1$; (**b**) $m = 2$. Here, the sizes of each plot in (**a**,**b**) are $220 \times 220\ \mu m^2$.

5. Conclusions

In conclusion, we have demonstrated the manipulation of the polarization states in the high-resolution focusing points and vector beams after passing a scattering medium. The VTM of a scattering medium is measured based on a four-step phase shift method and a 2D holographic grating. The simulation and experiment studies indicate that the constructed high-resolution focusing points and the vector beams with spatially variant states of polarization distribution through a scattering medium can be achieved based on the measured VTM. The experiment results of the intensity and polarization state distribution are in good agreement with that of the simulation. This work extends the vectorial manipulation and application of constructed high-resolution focusing points and vector beams through a scattering medium. Our findings will bring new research perspectives to the technologies related to high-resolution imaging, high-capacity optical communication, and optical manipulation in a scattering environment.

References

1. Pasquesi, J.J.; Schlachter, S.C.; Boppart, M.D.; Chaney, E.; Kaufman, S.J.; Boppart, S.A. In Vivo Detection of Exercise-Induced Ultra-structural Changes in Genetically-Altered Murine Skeletal Muscle Using Polarization-Sensitive Optical Coherence Tomography. *Opt. Express* **2006**, *14*, 1547–1556. [PubMed]
2. Rao, R.A.R.; Mehta, M.R.; Toussaint, K.C. Fourier Transform-Second-Harmonic Generation Imaging of Biological Tissues. *Opt. Express* **2009**, *17*, 14534–14542. [CrossRef]
3. Kotlyar, V.V.; Kovalev, A.A.; Zaitsev, V.D. Topological Charge of Light Fields with a Polarization Singularity. *Photonics* **2022**, *9*, 298. [CrossRef]
4. Zaltron, A.; Merano, M.; Mistura, G.; Sada, C.; Seno, F. Optical Tweezers in Single-Molecule Experiments. *Eur. Phys. J. Plus* **2020**, *135*, 896. [CrossRef]
5. Kozawa, Y.; Sato, S. Optical Trapping of Micrometer-Sized Dielectric Particles by Cylindrical Vector Beams. *Opt. Express* **2010**, *18*, 10828–10833. [CrossRef]
6. Meier, M.; Romano, V.; Feurer, T. Material Processing with Pulsed Radially and Azimuthally Polarized Laser Radiation. *Appl. Phys. A* **2007**, *86*, 329–334. [CrossRef]
7. Wang, H.; Shi, L.; Yuan, G.; Miao, X.; Tan, W.; Chong, T. Subwavelength and Super-Resolution Nondiffraction Beam. *Appl. Phys. Lett.* **2006**, *89*, 171102. [CrossRef]
8. Zhang, X.; Xia, T.; Cheng, S.; Tao, S. Free-Space Information Transfer Using the Elliptic Vortex Beam with Fractional Topolog ical Charge. *Opt. Commun.* **2019**, *431*, 238–244. [CrossRef]
9. Doronin, A.; Vera, N.; Staforelli, J.P.; Coelho, P.; Meglinski, I. Propagation of Cylindrical Vector Laser Beams in Turbid Tissue-Like Scattering Media. *Photonics* **2019**, *6*, 56. [CrossRef]
10. Huang, H.; Chen, Z.; Sun, C.; Liu, J.; Pu, J. Light Focusing through Scattering Media by Particle Swarm Optimi zation. *Chin. Phys. Lett.* **2015**, *32*, 104202. [CrossRef]
11. Popoff, S.M.; Lerosey, G.; Carminati, R.; Fink, M.; Boccara, A.C.; Gigan, S. Measuring the Transmission Matrix in Optics: An Approach to the Study and Control of Light Propagation in Disordered Media. *Phys. Rev. Lett.* **2010**, *104*, 100601. [CrossRef] [PubMed]
12. Popoff, S.; Lerosey, G.; Fink, M.; Boccara, A.C.; Gigan, S. Controlling Light through Optical Disordered Media: Transmission Matrix Approach. *New J. Phys.* **2011**, *13*, 123021. [CrossRef]
13. Conkey, D.B.; Caravaca-Aguirre, A.M.; Piestun, R. High-Speed Scattering Medium Characterization with Application to Fo cusing Light through Turbid Media. *Opt. Express* **2012**, *20*, 1733–1740. [CrossRef] [PubMed]
14. Hofer, M.; Brasselet, S. Manipulating the Transmission Matrix of Scattering Media for Nonlinear Imaging beyond the Memory Effect. *Opt. Lett.* **2019**, *44*, 2137–2140. [CrossRef] [PubMed]
15. Choi, Y.; Yang, T.D.; Fang-Yen, C.; Kang, P.; Lee, K.J.; Dasari, R.R.; Feld, M.S.; Choi, W. Overcoming the Diffraction Limit Using Multiple Light Scattering in a Highly Disordered Medium. *Phys. Rev. Lett.* **2011**, *107*, 023902. [CrossRef] [PubMed]
16. Lee, K.; Park, Y. Exploiting the Speckle-Correlation Scattering Matrix for a Compact Reference-Free Holographic Image Sensor. *Nat. Commun.* **2016**, *7*, 13359. [CrossRef] [PubMed]
17. Gong, C.; Shao, X.; Wu, T.; Liu, J.; Zhang, J. Total Variation Optimization for Imaging through Turbid Media with Transmission Matrix. *Opt. Eng.* **2016**, *55*, 121703. [CrossRef]
18. Yang, H.; Huang, Y.; Gong, C.; Wu, T.; Shao, X. Advances on Techniques of Breaking Diffraction Limitation Using Scattering Medium. *Chin. Opt.* **2014**, *7*, 1–25.
19. Liu, J.; Wang, J.; Li, W.; Sun, X.; Zhu, L.; Guo, C.; Shao, X. Programmable Multiwavelength Achromatic Focusing and Imaging through Scattering Media. *IEEE Photonics J.* **2018**, *10*, 6900811. [CrossRef]
20. Cui, M.; Yang, C. Implementation of a Digital Optical Phase Conjugation System and Its Application to Study the Robustness of Turbidity Suppression by Phase Conjugation. *Opt. Express* **2010**, *18*, 3444–3455. [CrossRef]
21. Lhermite, J.; Suran, E.; Kermène, V.; Louradour, F.; Desfarges-Berthelemot, A.; Barthélémy, A. Coherent Combining of 49 Laser Beams from a Multiple Core Optical Fiber by a Spatial Light Modulator. *Opt. Express* **2010**, *18*, 4783–4789. [CrossRef]

22. Bertolotti, J.; Van Putten, E.G.; Blum, C.; Lagendijk, A.; Vos, W.L.; Mosk, A.P. Non-Invasive Imaging through Opaque Scatter ing Layers. *Nature* **2012**, *491*, 232–234. [CrossRef]

23. Edrei, E.; Scarcelli, G. Optical Imaging through Dynamic Turbid Media Using the Fourier-Domain Shower-Curtain Effect. *Optica* **2016**, *3*, 71–74. [CrossRef]

24. Wang, X.; Jin, X.; Li, J.; Lian, X.; Ji, X.; Dai, Q. Prior-Information-Free Single-Shot Scattering Imaging beyond the Memory Effect. *Opt. Lett.* **2019**, *44*, 1423–1426. [CrossRef] [PubMed]

25. Vellekoop, I.M.; Lagendijk, A.; Mosk, A. Exploiting Disorder for Perfect Focusing. *Nat. Photonics* **2010**, *4*, 320–322. [CrossRef]

26. Choi, Y.; Hillman, T.R.; Choi, W.; Lue, N.; Dasari, R.R.; So, P.T.; Choi, W.; Yaqoob, Z. Measurement of the Time-Resolved Reflection Matrix for Enhancing Light Energy Delivery into a Scattering Medium. *Phys. Rev. Lett.* **2013**, *111*, 243901. [CrossRef] [PubMed]

27. Tripathi, S.; Paxman, R.; Bifano, T.; Toussaint, K.C. Vector Transmission Matrix for the Polarization Behavior of Light Propa gation in Highly Scattering Media. *Opt. Express* **2012**, *20*, 16067–16076. [CrossRef] [PubMed]

28. Xie, Y.-Y.; Wang, B.-Y.; Cheng, Z.-J.; Yue, Q.-Y.; Guo, C.-S. Measurement of Vector Transmission Matrix and Control of Beam Focusing through a Multiple-Scattering Medium Based on a Vector Spatial Light Modulator and Two-Channel Polarization Holography. *Appl. Phys. Lett.* **2017**, *110*, 221105. [CrossRef]

29. Yu, P.; Zhao, Q.; Hu, X.; Li, Y.; Gong, L. Tailoring Arbitrary Polarization States of Light through Scattering Media. *Appl. Phys. Lett.* **2018**, *113*, 121102. [CrossRef]

30. Zhao, Q.; Tu, S.; Lei, Q.; Guo, C.; Zhan, Q.; Cai, Y. Creation of Cylindrical Vector Beams through Highly Anisotropic Scattering Media with a Single Scalar Transmission Matrix Calibration. *Photonics Res.* **2022**, *10*, 1617–1623. [CrossRef]

31. MacKintosh, F.C.; Zhu, J.-X.; Pine, D.; Weitz, D. Polarization Memory of Multiply Scattered Light. *Phys. Rev. B* **1989**, *40*, 9342. [CrossRef] [PubMed]

32. Shumyatsky, P.; Milione, G.; Alfano, R.R. Optical Memory Effect from Polarized Laguerre–Gaussian Light Beam in Light-Scattering Turbid Media. *Opt. Commun.* **2014**, *321*, 116–123. [CrossRef]

33. Liu, C.; Zhu, H.; Chen, R.-P.; Dai, C.-Q.; He, S. Polarization Evolution of a Vector Vortex Optical Field in a Strongly Nonlocal Nonlinear Medium. *IEEE Photonics J.* **2019**, *11*, 6101210. [CrossRef]

34. Xie, Y.-Y. Study on Wavefront Control and Application of Vector Beams. Ph.D. Thesis, Shandong Normal University, Jinan, China, 2017.

35. Stary, M.; Novotny, F.; Horak, M.; Stara, M.; Hotar, V.; Matusek, O. Summary of the Properties and Benefits of Glass Mechanically Frosted with an Abrasive Brush. *Constr. Build. Mater.* **2019**, *206*, 364–374. [CrossRef]

36. Chen, R.-P.; Chen, Z.; Chew, K.-H.; Li, P.-G.; Yu, Z.; Ding, J.; He, S. Structured Caustic Vector Vortex Optical Field: Manipu lating Optical Angular Momentum Flux and Polarization Rotation. *Sci. Rep.* **2015**, *5*, 10628. [CrossRef] [PubMed]

37. Chen, H.; Hao, J.; Zhang, B.-F.; Xu, J.; Ding, J.; Wang, H.-T. Generation of Vector Beam with Space-Variant Distribution of Both Polarization and Phase. *Opt. Lett.* **2011**, *36*, 3179–3181. [CrossRef]

38. Van Putten, E.G.; Akbulut, D.; Bertolotti, J.; Vos, W.L.; Lagendijk, A.; Mosk, A. Scattering Lens Resolves Sub-100 Nm Structures with Visible Light. *Phys. Rev. Lett.* **2011**, *106*, 193905. [CrossRef] [PubMed]

39. Galaktionov, I.; Nikitin, A.; Sheldakova, J.; Toporovsky, V.; Kudryashov, A. Focusing of a Laser Beam Passed through a Mod erately Scattering Medium Using Phase-Only Spatial Light Modulator. *Photonics* **2022**, *9*, 296. [CrossRef]

40. Zheng, S.; Yang, W.; Situ, G. Application of Computational Optical Imaging in Scattering. *Infrared Laser Eng.* **2019**, *48*, 603005. [CrossRef]

41. Sun, C.; Zhao, Y.; An, Z.; Fu, Q.; Zhan, J.; Duan, J. Effect of Concentration on Propagation Characteristics of Polarized Laser in Oil-Mist Diffusion. *J. Appl. Opt.* **2017**, *38*, 6.